Microporous Polypropylene Sheets Containing $CaCO_3$ Filler: Effects of Stretching Ratio and Removing $CaCO_3$ Filler

SATOSHI NAGŌ, YUKIO MIZUTANI

Tokuyama Corp., Tokuyama City, Yamaguchi 745, Japan

Received 3 December 1996; accepted 5 April 1997

ABSTRACT: Microporous polypropylene sheets are prepared by biaxially stretching polypropylene sheets containing $CaCO_3$ filler. Here, the stretching ratio is one of the most important factors in the preparative process, and removing the $CaCO_3$ filler also affects the sheet properties. Their effects were studied in relation to the properties and the structure of the microporous polypropylene sheets. © 1998 John Wiley & Sons, Inc. J Appl Polym Sci 68: 1543–1553, 1998

Key words: microporous polypropylene sheets; $CaCO_3$ filler; biaxial stretching; stretching ratio; porous structure

INTRODUCTION

We reported on microporous polypropylene (PP) sheets prepared by biaxially stretching PP sheets containing $CaCO_3$ filler, and it is elucidated that the filler content, the size of filler particles, the draft ratio, and the stretching ratio are important factors in relation to the sheet properties.[1–5] Also, we reported some structural changes of microporous PP sheets by the biaxial stretching: stretching in machine direction (MD) and subsequent stretching in transverse direction (TD).[2]

In this article, we report the changes of some properties and the structure of microporous PP sheets, mainly by investigating their N_2 gas permeability and also with the aid of scanning electron microscopy.

EXPERIMENTAL

Materials

PP powder was PN-120 from Tokuyama Corp. (MFI, 1.7). $CaCO_3$ was of commercial grade (0.08 μm particle size in diameter). Liquid polyester composed of adipic acid and poly(propylene glycol) (average molecular weight, 2300) was used as an additive. The antioxidant used was 2,6-di-*t*-butyl-4-methylphenol of commercial grade.

Preparation

PP powder (40 wt %), $CaCO_3$ filler (60 wt %), the antioxidant (1.3 wt % of PP), and the additive (2 wt % of $CaCO_3$ filler) were well mixed in advance. The resultant mixture was extruded at 230°C to prepare pellet, which was extruded to mold base sheet. This base sheet was stretched at 90°C in MD (6.0 stretching ratio) by using two pairs of rollers with different rotating speeds and, subsequently, at 120°C in TD by using a biaxial stretching machine of pantagraph type (Type I, Brückner Co., Germany). Thus, microporous PP sheets were prepared, and the $CaCO_3$ filler was also removed by treating with a mixed solution of 1*N* HCl aqueous solution–CH_3OH (1 : 1 by volume) at room temperature overnight with stirring.

Measurement

Scanning Electron Microscopy

The surface and cross section of microporous PP sheet was observed with the aid of a scanning elec-

Correspondence to: S. Nagō.

Journal of Applied Polymer Science, Vol. 68, 1543–1553 (1998)
 CCC 0021-8995/98/101543-11

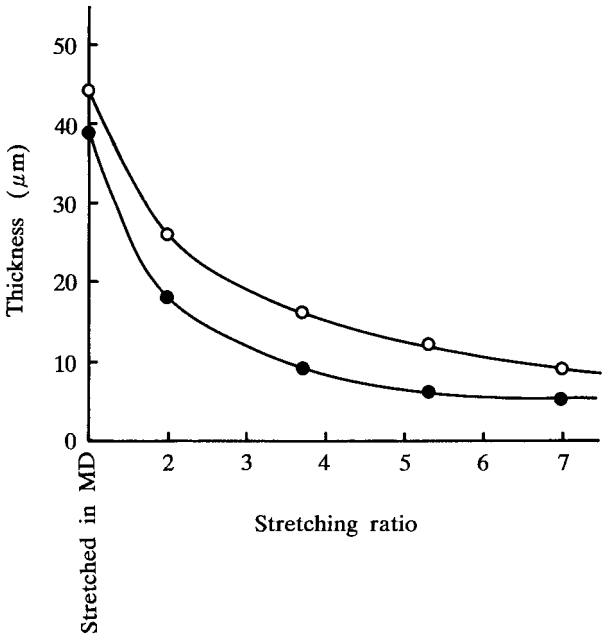

Figure 1 TD stretching ratio versus sheet thickness: (○) before the HCl treatment; (●) after the HCl treatment.

tron microscope, JSM-220, from JEOL Ltd. (Japan). The accelerated voltage and the probe current were 15 kV and 5 mA, respectively. Pretreatment of each sample was carried out with gold ion sputtering for 3 min at 1.2 kV and 8–10 mA.

Porosity

Apparent specific gravities of the base sheet (d_0) and the microporous PP sheet (d) were estimated by buoyancy method in water, and the porosity of the microporous sheet was calculated by the following equation:

$$\text{Porosity}\ (\%) = (d_0 - d)/d_0 \qquad (1)$$

Maximum Pore Size

The sample impregnated with methanol was set onto a cell, as shown elsewhere.[6] A small amount of methanol was filled over the sample surface, and N_2 gas pressure was increased at the rate of 1 kg cm^{-2} per min.

When three continuous bubbles were generated through the sample, N_2 gas pressure (P_j, kg cm^{-2}) was measured. Next, maximum pore size (D_{max}) was calculated by the following equation (ASTM F-316):

$$D_{max}(\mu\text{m}) = 0.9388 P_j^{-1} \qquad (2)$$

N_2 Gas Permeability

The sample was set between flanges sealed with rubber packing at an effective diameter of 20 mm, as shown elsewhere.[6] N_2 gas was supplied into the chamber through a pressure regulator (accuracy, 0.02 kg cm^{-2}). N_2 gas flux (J) was measured at 20°C by a digital flow meter, Model 2500SS, from Sōgō Rikagaku Industry Co. (Japan). Mean pressure ($\bar{P}$, kg cm^{-2}) was calculated by the following equation:

$$\bar{P} = (P_i + P_o)/2 \qquad (3)$$

where P_i and P_o are inlet and outlet pressure, respectively, and P_o is the atmospheric pressure.

Determination of Pore Structure

The micropore structure of the PP sheets was studied by measuring the N_2 gas permeability, as shown elsewhere.[6] Yasuda and Tsai[7] and Cabasso et al.[8] studied gas permeation through various millipore filters and polysulfone membrane and derived the following equations:

$$J = K\Delta P l^{-1} \qquad (4)$$

where J is N_2 gas flux (cm^3 cm^{-2} s^{-1}); K, the permeability coefficient (cm^2 s^{-1}); ΔP, the pressure difference across the sample (kg cm^{-2}); and l, the thickness of a sample (cm). The gas permeability coefficient (K) is determined as follows:

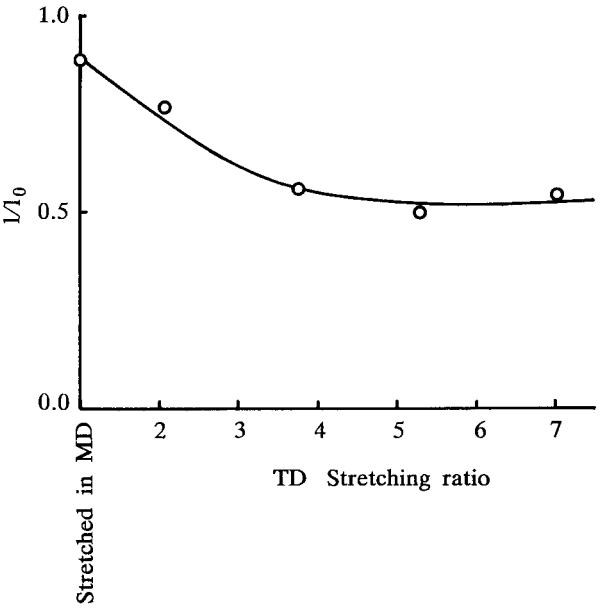

Figure 2 TD stretching ratio versus l/l_0: l, sheet thickness after the HCl treatment; l_0, sheet thickness before the HCl treatment.

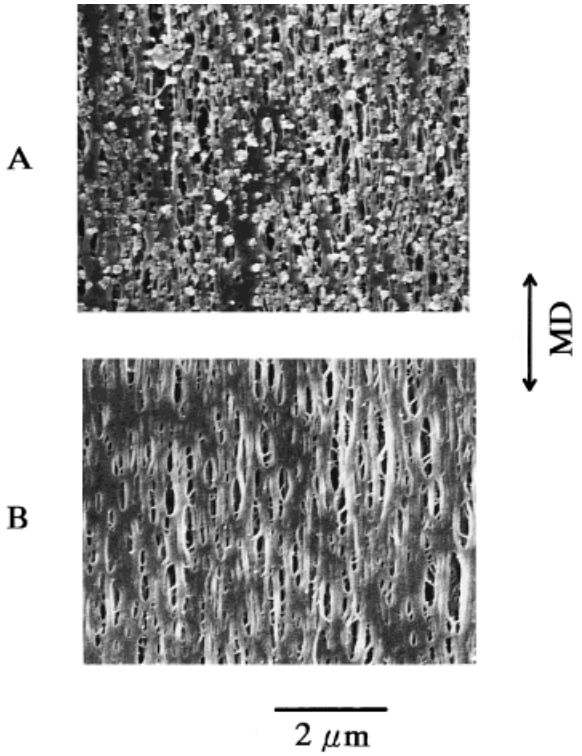

Figure 3 Scanning electron micrographs of surfaces of microporous PP sheet after stretching in MD: (A) before the HCl treatment; (B) after the HCl treatment.

$$K = lP_0Q(A\Delta P)^{-1} \quad (5)$$

where Q is volume flow rate of N_2 gas ($cm^3\ s^{-1}$), and A is the effective area of the sample (6.6 cm^2).

The permeability coefficient (K) of a microporous sheet can be shown as follows:

$$K = K_0 + B_0\eta^{-1}\bar{P} \quad (6)$$

where K_0 is the Knudsen permeability coefficient ($cm^2\ s^{-1}$); B_0, the geometric factor of the sheet (cm^2); and η, the viscosity of N_2 gas (1.75×10^{-4} dyne s cm^{-2} at 20°C). K_0 and B_0 can be estimated from the plot of K to $\bar{P}$.

The porosity of the sheet (ε) and tortuosity factor of pore (q) can be related to K_0 and B_0 as follows:

$$K_0 = (4/3)(\delta/k_1)(v/q^2)\varepsilon m \quad (7)$$

$$B_0 = (m^2/k)(\varepsilon/q^2) \quad (8)$$

where δ/k_1 and k are constants (0.8 and 2.5, respectively), as estimated by Carman[9]; and m is the equivalent pore size, as shown below.

The average molecular velocity of a gas (v; molecular weight, M) is shown as follows:

$$\bar{v} = (8RT/\pi M)^{0.5} \quad (9)$$

The equivalent pore size (m) can be calculated by combining eqs. (7)–(9):

$$m = (16/3)(B_0/K_0)(2RT/\pi M)^{0.5} \quad (10)$$

Thus, eq. (11) can be derived for measurement with N_2 gas at 20°C:

$$m = 1.256 \times 10^5(B_0/K_0) \quad (11)$$

Furthermore, the following equations are derived from eqs. (7) and (9) to estimate effective porosity (ε/q^2) and tortuosity factor of pore (q):

$$\varepsilon/q^2 = 2.5B_0/m^2 \quad (12)$$

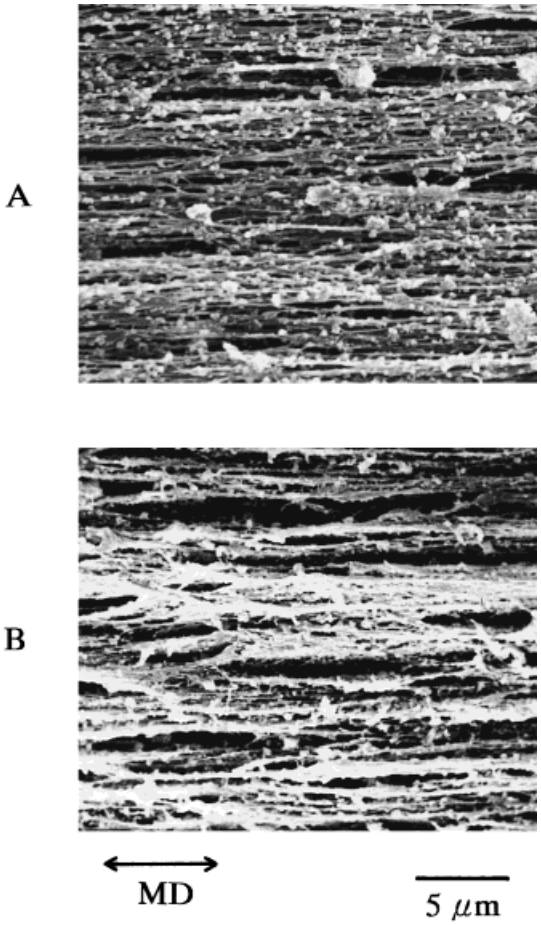

Figure 4 Scanning electron micrographs of cross sections of microporous PP sheet after stretching in MD: (A) before the HCl treatment; (B) after the HCl treatment.

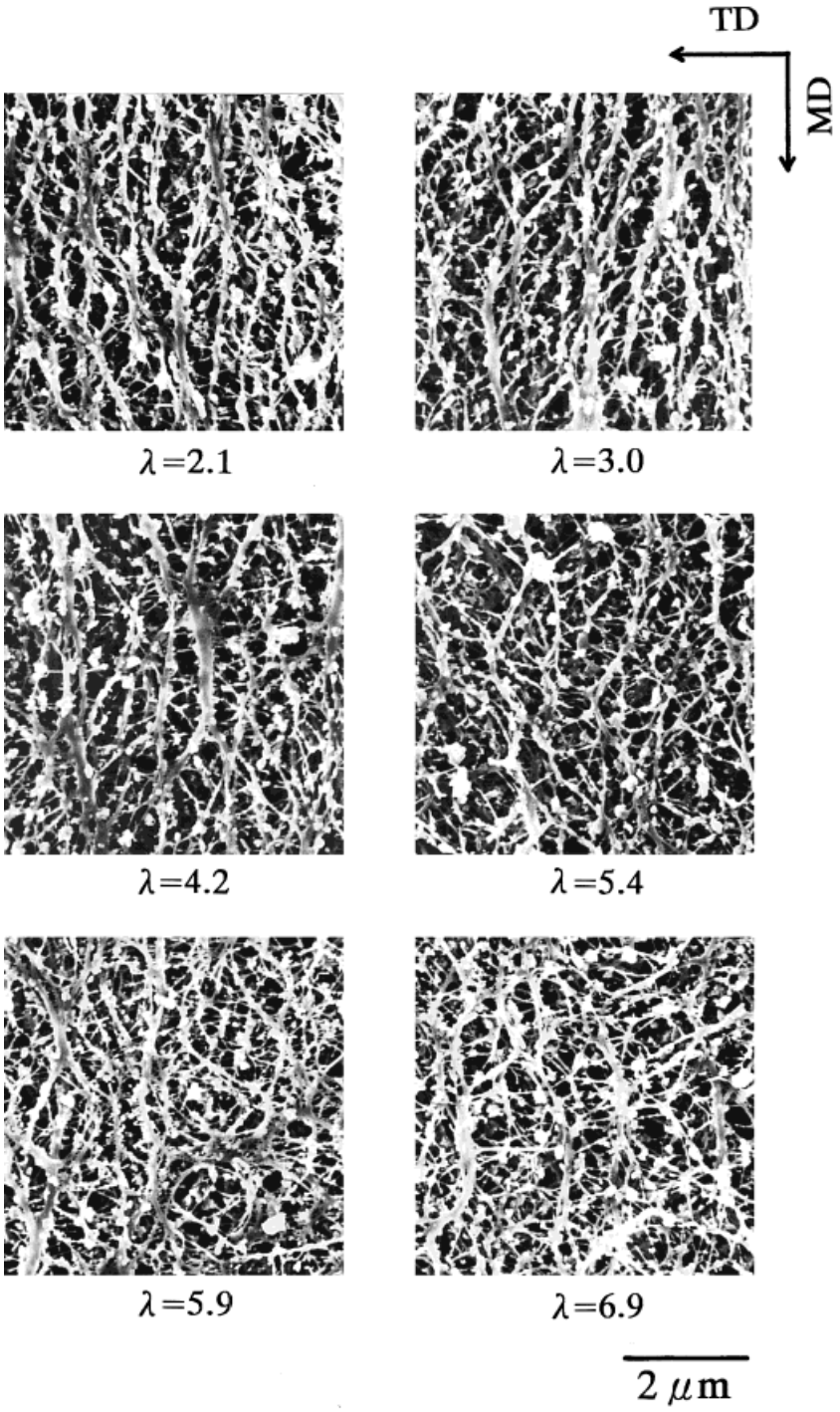

Figure 5 Scanning electron micrographs of surfaces of microporous PP sheet stretched in TD with various stretching ratio (λ) before the HCl treatment.

$$q = 0.63m(\varepsilon/B_0)^{0.5} \qquad (13)$$

RESULTS AND DISCUSSION

Microporous PP sheets are prepared by biaxially stretching PP sheets containing $CaCO_3$ filler. The PP phase is split at the periphery of the filler particles by stretching in MD, and the resultant voids are widened by subsequent stretching in TD. Thus, the PP sheets containing $CaCO_3$ filler are transformed to the microporous PP sheets. We mainly investigated the stretching effect in TD in this article.

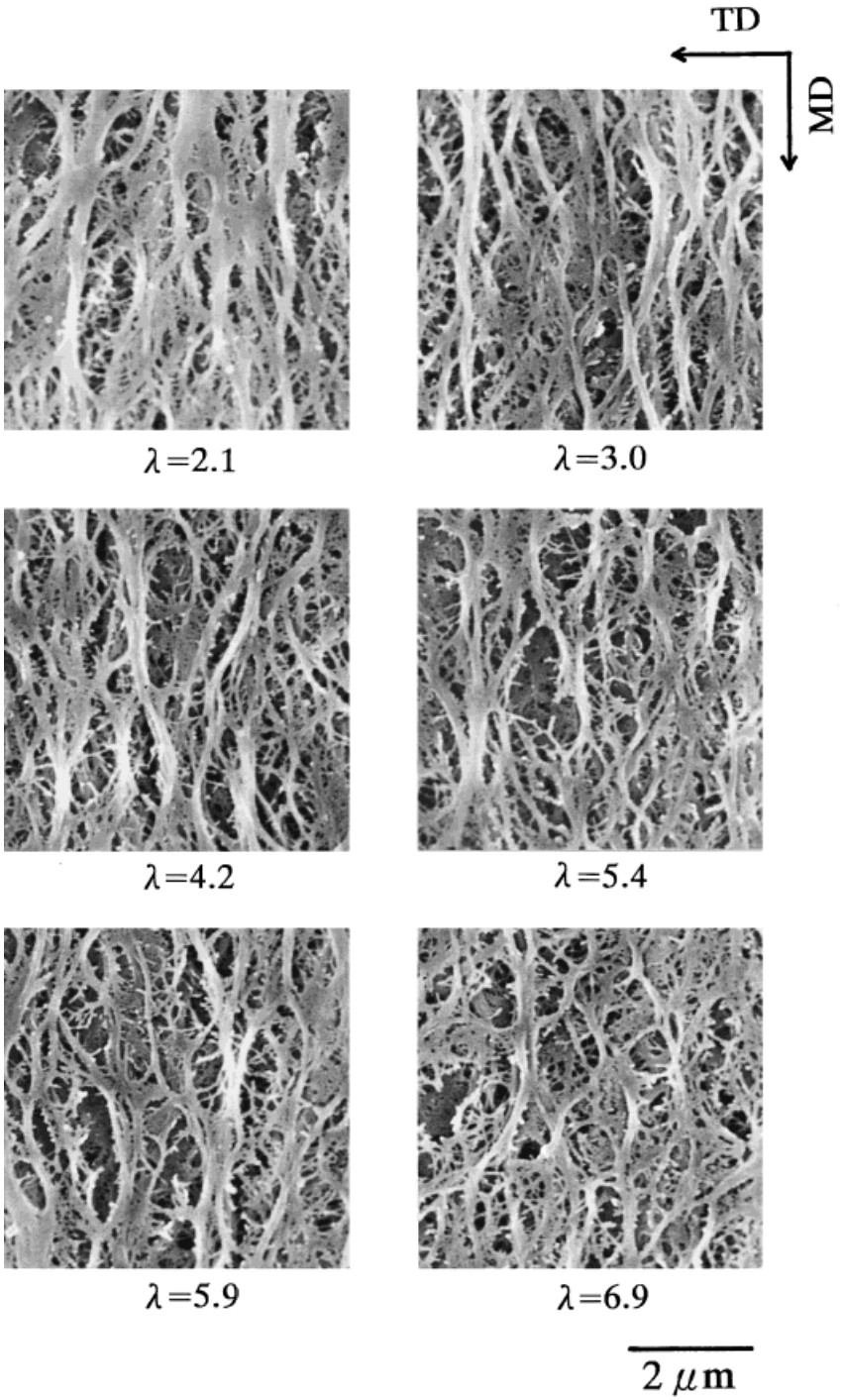

Figure 6 Scanning electron micrographs of surfaces of microporous PP sheet stretched in TD with various stretching ratio (λ) after the HCl treatment.

Figure 1 shows the stretching effect on the sheet thickness. The microporous PP sheet becomes thinner with an increase in the stretching ratio in both the cases before and after the HCl treatment. The sheet thickness after the HCl treatment is smaller than that before, due to removal of the filler particles as a spacer. Figure 2 shows the effect of removing the filler particles on the sheet thickness. The l/l_0 value decreases with increasing the stretching ratio. The tendency shown in Figure 1 means that the stretched PP phase becomes thinner with an increase in the stretching ratio. Accordingly, the result is understandable, considering that the participation of

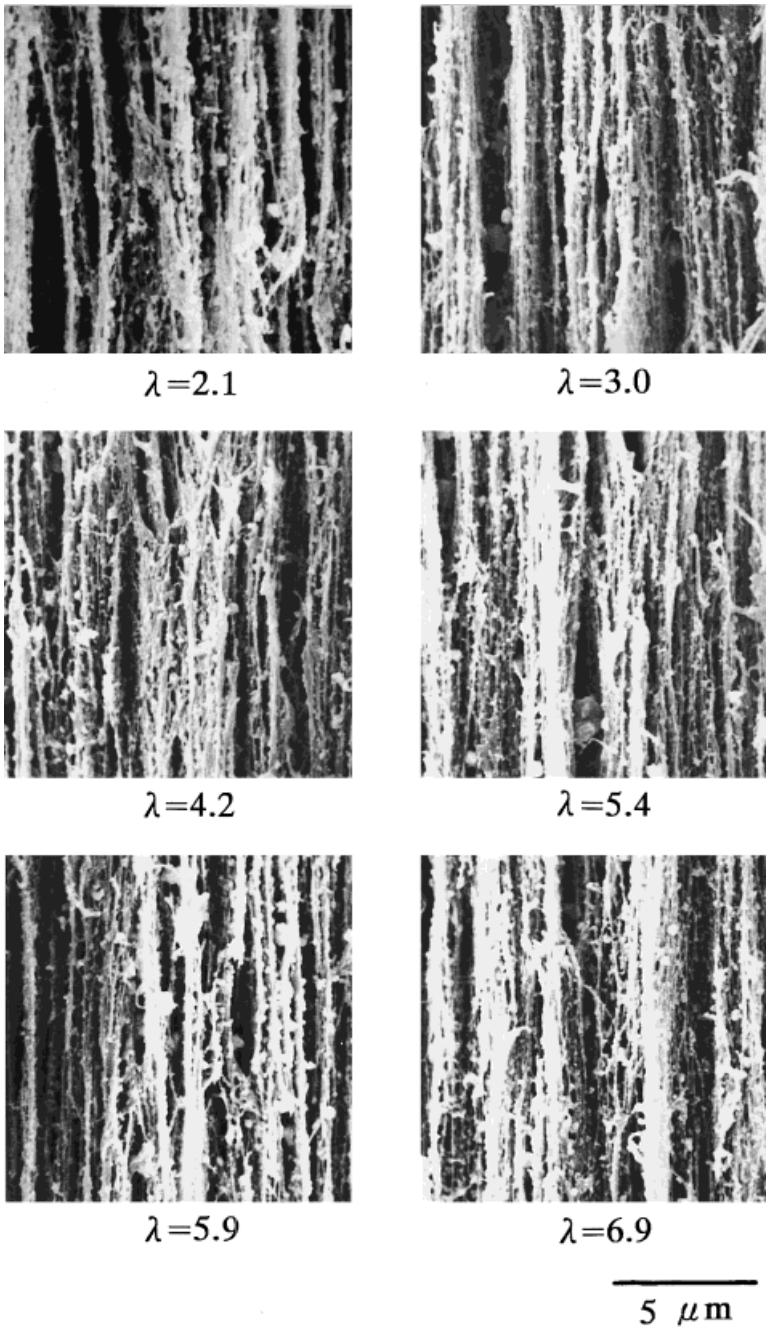

Figure 7 Scanning electron micrographs of cross sections of microporous PP sheet stretched in TD with various stretching ratios (λ) before the HCl treatment.

the filler particles in the sheet thickness is unchanged by the stretching. Here, it is noteworthy that almost all the filler particles were removed by the HCl treatment, estimated by the weight changes of microporous PP sheets before and after the HCl treatment; although a small number of the filler particles are observed in the fibrous PP texture after the HCl treatment, as will be shown later.

Scanning Electron Microscopy

Figures 3 and 4 show the surfaces and cross sections of microporous PP sheet stretched in MD (stretching ratio, 6), respectively. The removal of the filler particles makes it easier to observe the fibrous PP texture.

There are many long eliptical voids parallel to MD in the surfaces, and the relatively thicker PP

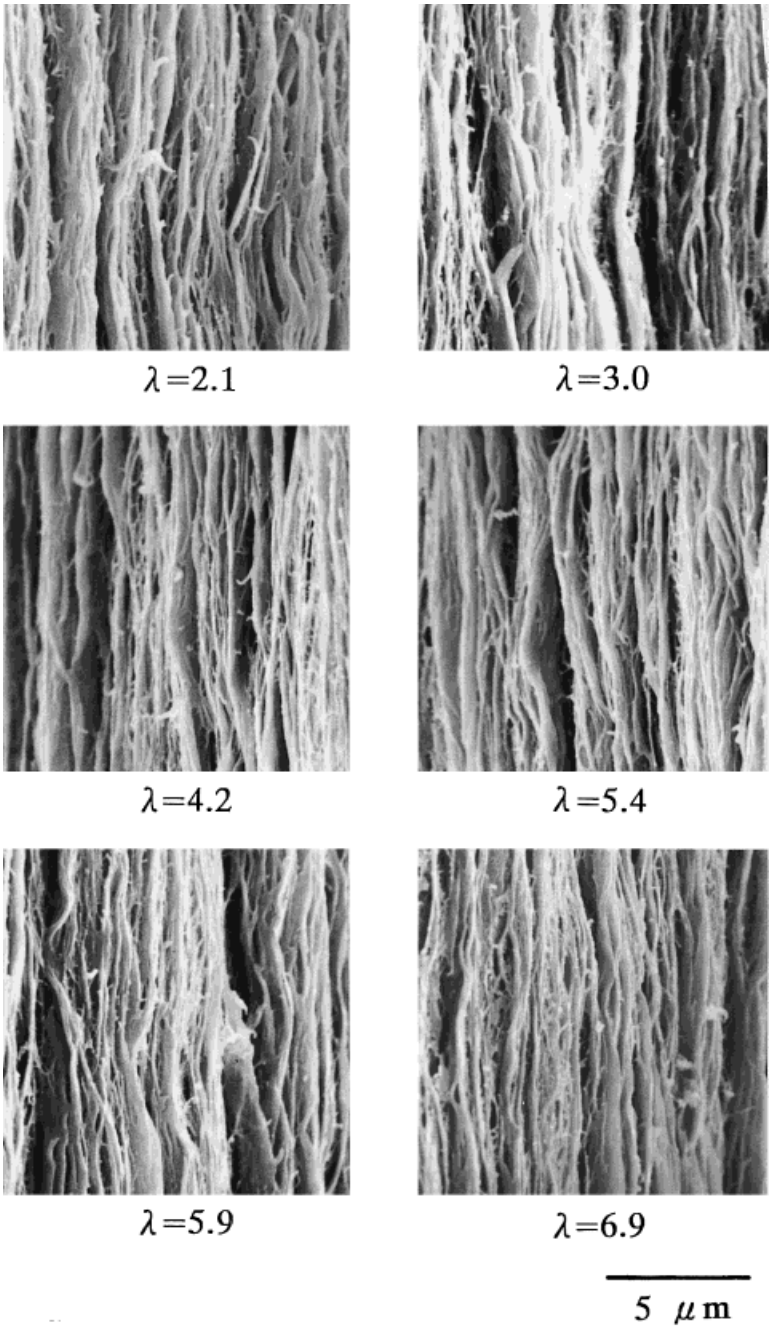

Figure 8 Scanning electron micrographs of cross sections of microporous PP sheet stretched in TD with various stretching ratios (λ) after the HCl treatment.

fibrils are orientated in MD. On the other hand, the layered structure of the PP fibrils parallel to the surface is observed in the cross sections.

Figures 5 and 6 show the surfaces of microporous PP sheets subsequently stretched in TD before and after the HCl treatment, respectively. The long eliptical voids in Figure 3 are widened in TD, and there are some relatively thicker PP fibrils orientated in MD, even when the stretching ratio equals 6.9. Also, the larger the stretching ratio, the much more the relatively finer fibrous PP texture is developed, which results from the splitting of the relatively thicker PP fibrils orientated in MD. It is interesting that the PP fibrils orientated in MD are thicker than the others, and this suggests that the stretching in MD is pretty effective regarding the splitting of the PP phase.

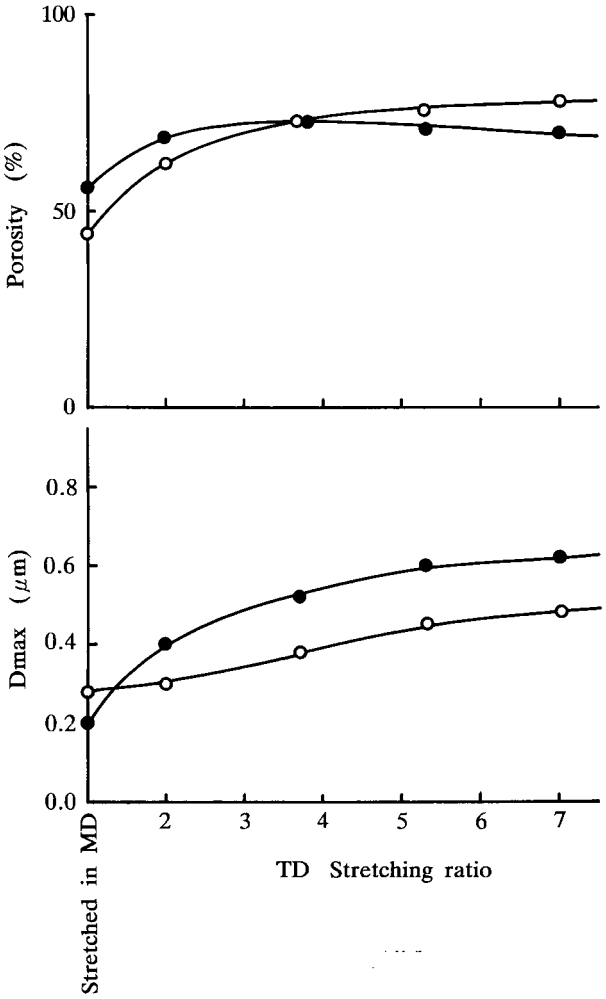

Figure 9 TD stretching ratio versus porosity and D_{max}: (○) before the HCl treatment; (●) after the HCl treatment.

Figures 7 and 8 show the cross sections stretched in TD before and after the HCl treatment, respectively. The layered structure of fibrous PP texture is observed in all the cases, and its dependency onto the stretching ratio is rather obscure.

Properties of Microporous PP Sheets

Figure 9 shows the stretching effect on porosity and the D_{max} of microporous PP sheets. Before the HCl treatment, the porosity gradually increases with an increase in the stretching ratio. It is reasonable in consideration of the widening of the pore by the stretching, as shown in Figure 5. On the other hand, after removing the filler particles, the porosity increases once, then slightly decreases. The increase is due to removal of the filler particles when the stretching ratio is relatively smaller, and the slight decrease is due to compaction of the fibrous PP texture caused by the removal of the filler particles as a spacer. D_{max} becomes larger with an increase in the stretching ratio in both the cases before and after the HCl treatment. In the case after the HCl treatment, D_{max} is larger than those in the case of before the HCl treatment and increases with an increase in the stretching ratio, although the porosity is smaller than those in the case before the HCl treatment and then decreases over the stretching ratio equal to 4. This means that the widening of the pore by the stretching and removing the filler particles is dominant in relation to D_{max}.

Structure of Microporous PP Sheets

Figures 10 and 11 show the effect of the pressure difference on N_2 gas flux through microporous PP sheets before and after the HCl treatment, respectively. The larger the stretching ratio, the larger the N_2 gas flux. The linear relations are obtained in both cases. Then the permeability coefficients are estimated from Figures 10 and 11 by using eq. (4).

Figures 12 and 13 show the relations between the mean pressure and the permeability coefficient in the cases before and after the HCl treatment, respectively. The linear relations are ob-

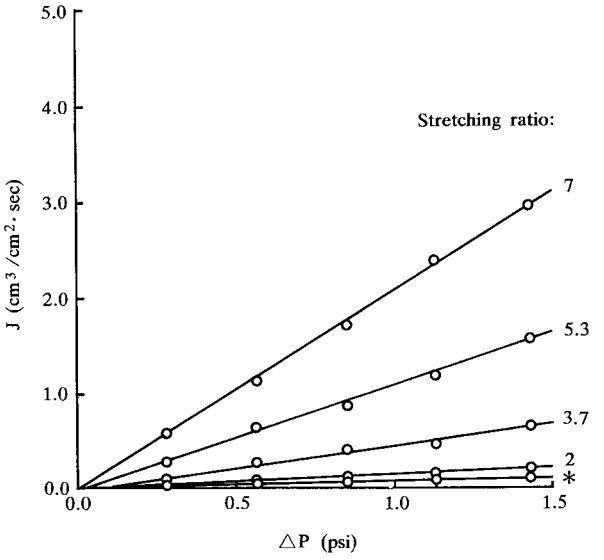

Figure 10 ΔP versus J before the HCl treatment: (*) stretched only in MD.

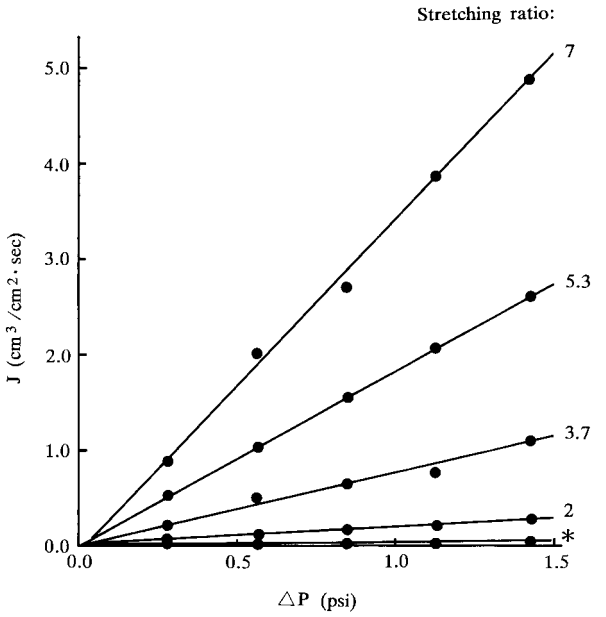

Figure 11 ΔP versus J after the HCl treatment: (*) stretched only in MD.

tained in both the cases. Next, Knudsen permeability coefficients and geometric factors can be estimated from the intercepts on vertical axis and the slopes of the linear lines, respectively.

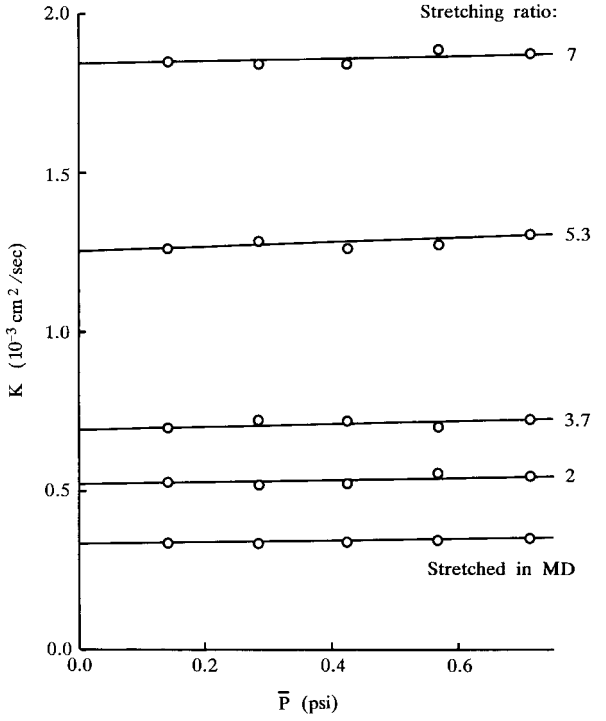

Figure 12 $\bar{P}$ versus K before the HCl treatment.

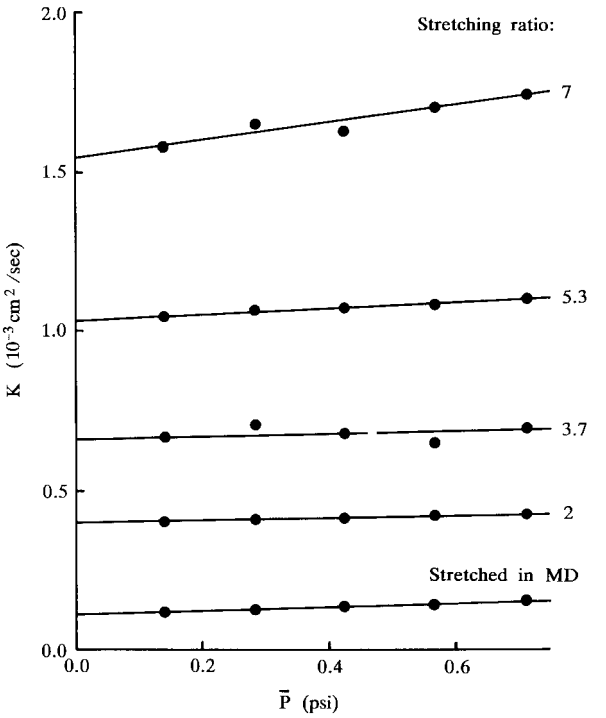

Figure 13 $\bar{P}$ versus K after the HCl treatment.

Figure 14 show the dependencies of the geometric factor and the Knudsen permeability onto the stretching ratio in the cases before and after the HCl treatment. The larger the stretching ratio, the larger the geometric factor and the Knudsen permeability coefficient. It is interesting that both the geometric factor and the Knudsen permeability coefficient in the case before the HCl treatment once decreased at the stretching ratio equal to 2 due to widening of microvoids by the stretching in TD in the presence of the $CaCO_3$ filler particles.

Figure 15 shows the effects of the stretching ratio onto the effective porosity, tortuosity factor of the pore, and the pore size. The larger the stretching ratio, the larger the pore size in both the cases before and after the HCl treatment. In the case before the HCl treatment, the relatively larger decrease of the tortuosity factor at the stretching ratio equal to 2 is ascribed to the stretching in TD, which causes the widening of the microvoids resulted by the stretching in MD, as described before; and then further stretching makes the tortuosity factor slightly decreased. However, the tortuosity factors are pretty large. The effective porosity increases with an increase in the stretching ratio, and the

values are pretty small. These results suggest that the fibrous PP texture is complicated. Furthermore, the comparison of the values after the HCl treatment with those before suggests the interesting role of the $CaCO_3$ filler particles as a spacer. Namely, the removal of the $CaCO_3$ filler particles, a hindering material in other words increases the pore sizes in comparison with those before the HCl treatment but causes the compaction of the PP fibrils, which makes the effective porosity and the tortuosity factor smaller and larger in the case after the HCl treatment than those in the case before the treatment, respectively. These tendencies mean that the removal of the $CaCO_3$ filler particles makes the sheet structure relatively more compact.

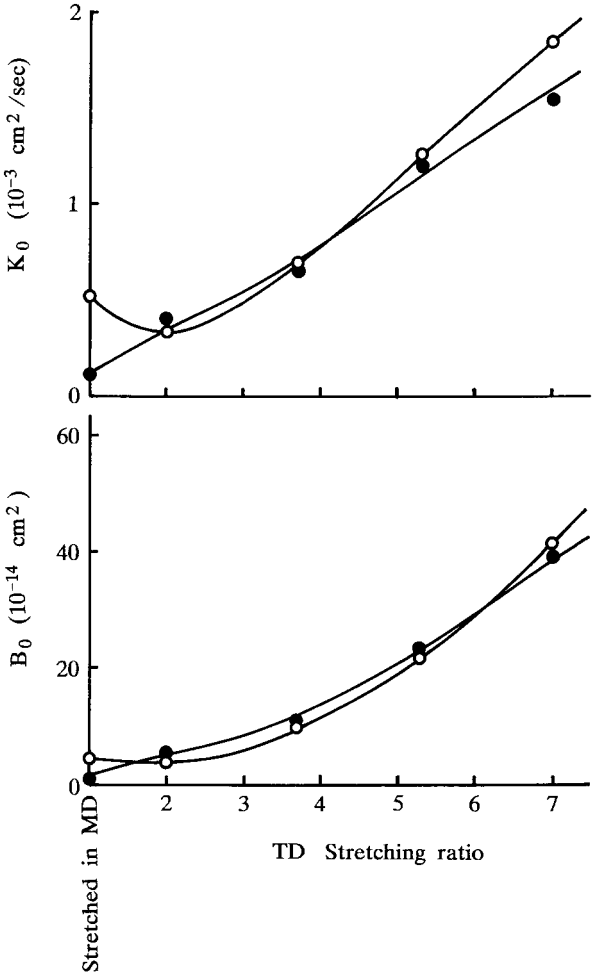

Figure 14 TD stretching ratio versus K_0 and B_0: (○) before the HCl treatment; (●) after the HCl treatment.

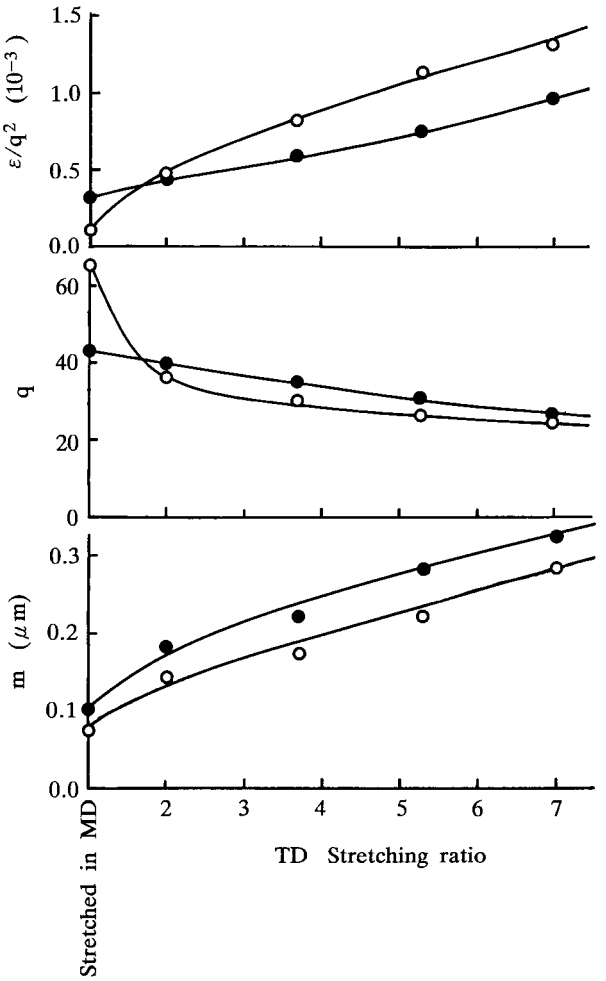

Figure 15 TD stretching ratio versus ε/q^2, q, and m: (○) before the HCl treatment; (●) after the HCl treatment.

CONCLUSION

Microporous PP sheets are prepared by biaxially stretching PP sheets containing $CaCO_3$ filler particles: stretching in MD and subsequent stretching in TD. With the aid of scanning electron microscopy and measurement of N_2 gas permeability, we mainly investigated the effects of the stretching in TD on some properties (porosity and D_{max}) and the structural change. Also, we similarly investigated the effects of removing $CaCO_3$ filler particles by the HCl treatment. The stretching in TD makes the fibrous PP texture finer: fibrils with round pores in the surface and layered structure in the cross section. The estimated values of the tortuosity factor and the effective porosity suggest that the fibrous PP texture is pretty complex and that the details should be studied further.

REFERENCES

1. S. Nakamura, K. Okamura, S. Kaneko, and Y. Mizutani, *Kobunshi Ronbunshu,* **48,** 463 (1991).
2. S. Nagō, S. Nakamura, and Y. Mizutani, *J. Electron Microsc.,* **41,** 107 (1992).
3. Y. Mizutani, S. Nakamura, S. Kaneko, and K. Okamura, *Ind. Eng. Chem. Res.,* **32,** 221 (1993).
4. S. Nakamura, S. Kaneko, and Y. Mizutani, *J. Appl. Polym. Sci.,* **49,** 143 (1993).
5. S. Nagō and Y. Mizutani, *J. Appl. Polym. Sci.,* **61,** 31 (1996).
6. S. Nagō, S. Nakamura, and Y. Mizutani, *J. Appl. Polym. Sci.,* **45,** 1527 (1992).
7. H. Yasuda and J. T. Tsai, *J. Appl. Polym. Sci.,* **18,** 805 (1974).
8. I. Cabasso, K. Q. Robert, E. Klein, and J. K. Smith, *J. Appl. Polym. Sci.,* **21,** 1883 (1977).
9. P. G. Carman, *Flow of Gas through Porous Media,* Butterworth, London, 1956.